the FEBS Journal

Proteomic analysis of dopamine and α-synuclein interplay in a cellular model of Parkinson's disease pathogenesis

Tiziana Alberio[1], Alessandra Maria Bossi[2], Alberto Milli[2], Elisa Parma[1], Marzia Bruna Gariboldi[1], Giovanna Tosi[3], Leonardo Lopiano[4] and Mauro Fasano[1]

1 Department of Structural and Functional Biology, and Centre of Neuroscience, University of Insubria, Busto Arsizio, Italy
2 Department of Biotechnology, University of Verona, Italy
3 Department of Clinical and Biological Sciences, University of Insubria, Varese, Italy
4 Department of Neuroscience, University of Torino, Italy

Keywords
dopamine; network enrichment; NF-κB; Parkinson's disease; SH-SY5Y; α-synuclein

Correspondence
M. Fasano, Department of Structural and Functional Biology, and Centre of Neuroscience, University of Insubria, via Alberto da Giussano 12, 21052 Busto Arsizio, Italy
Fax: +39 0331 339459
Tel: +39 0331 339450
E-mail: mauro.fasano@uninsubria.it
Website: http://busto.dipbsf.uninsubria.it/cns/fasano/

(Received 4 June 2010, revised 14 July 2010, accepted 27 September 2010)

doi:10.1111/j.1742-4658.2010.07896.x

Altered dopamine homeostasis is an accepted mechanism in the pathogenesis of Parkinson's disease. α-Synuclein overexpression and impaired disposal contribute to this mechanism. However, biochemical alterations associated with the interplay of cytosolic dopamine and increased α-synuclein are still unclear. Catecholaminergic SH-SY5Y human neuroblastoma cells are a suitable model for investigating dopamine toxicity. In the present study, we report the proteomic pattern of SH-SY5Y cells overexpressing α-synuclein (1.6-fold induction) after dopamine exposure. Dopamine itself is able to upregulate α-synuclein expression. However, the effect is not observed in cells that already overexpress α-synuclein as a consequence of transfection. The proteomic analysis highlights significant changes in 23 proteins linked to specific cellular processes, such as cytoskeleton structure and regulation, mitochondrial function, energetic metabolism, protein synthesis, and neuronal plasticity. A bioinformatic network enrichment procedure generates a significant model encompassing all proteins and allows us to enrich functional categories associated with the combination of factors analyzed in the present study (i.e. dopamine together with α-synuclein). In particular, the model suggests a potential involvement of the nuclear factor kappa B pathway that is experimentally confirmed. Indeed, α-synuclein significantly reduces nuclear factor kappa B activation, which is completely quenched by dopamine treatment.

Introduction

Parkinson's disease (PD) is a sporadic neurodegenerative disorder of unknown etiology characterized mainly by the progressive degeneration of dopaminergic neurons of the substantia nigra pars compacta (SNpc) and depletion of striatal dopamine. Dopaminergic neuronal death is accompanied by the appearance of Lewy bodies (LB), intracytoplasmic inclusions immunoreactive for α-synuclein, ubiquitin, 3-nitrotyrosine and neurofilament [1,2]. Many of the genetic factors variously associated with PD, such as α-synuclein mutations and

Abbreviations
α-syn, human α-synuclein overexpressing cells; β-gal, β-galactosidase expressing cells; C1qBP, C1Q binding protein; CRMP4, collapsin response mediator protein 4; 2-DE, 2D electrophoresis; eIF5A, eukaryotic initiation factor 5A; GAPDH, glyceraldehyde-3-phosphate dehydrogenase; GO, Gene Ontology; GSK-3β, glycogen synthase kinase 3β; GSTπ, glutathione *S*-transferase π; LB, Lewy bodies; MTT, 3-(4,5-dimethylthiazol-2-yl)-2,5-diphenyltetrazolium bromide; NF-κB, nuclear factor kappa B; PD, Parkinson's disease; Ran1BP, Ran 1 binding protein; RPLP2, 60S acidic ribosomal protein P2; SNpc, substantia nigra pars compacta; VDAC-2, voltage-dependent anion channel 2.

overexpression, parkin and PTEN-induced putative kinase 1 loss-of-function and UCHL1 mutation, lead to an impairment of neuronal dopamine homeostasis by interfering with the vesicular storage and release mechanisms. Dopamine auto-oxidation in the cytosol determines oxidative stress conditions that are magnified by impairment of the antioxidant defense of the cell, as in the case of DJ-1 or PTEN-induced putative kinase 1 mutations. Mitochondrial and proteasome dysfunction and oxidative stress could account for the selective degeneration of dopaminergic SNpc neurons and their specific vulnerability [1–6].

Single point mutations in α-synuclein, as well as duplication and triplication of the gene, were reported to be linked with rare familial forms of PD [6]. However, α-synuclein deposition into LB is a general hallmark of the PD state, suggesting that the accumulation of α-synuclein might cause selective degeneration of dopaminergic neurons [1,4]. Expression of either wild-type or mutant protein in different cell lines demonstrated that α-synuclein modulates dopamine toxicity, which was associated with reactive oxygen species arising from dopamine oxidation [3,4]. Nevertheless, the normal function of α-synuclein is poorly understood and α-synuclein expressed at low levels appears to be neuroprotective and anti-apoptotic, indicating a dual role for this protein [7–9]. Several lines of evidence suggest that the upregulation of α-synuclein represents a compensatory mechanism adopt by neurons to protect themselves from chronic oxidative stress [9,10].

In the present study, we investigate the dopamine effect on the expression pattern of cellular proteins in the human catecholaminergic neuroblastoma cell line SH-SY5Y, overexpressing α-synuclein. A proteomic analysis is expected to identify cellular alterations that are associated with dopamine treatment and modulated by α-synuclein overexpression, without any *a priori* hypothesis [4,11,12]. SH-SY5Y cells couple good dopamine transporter activity with a low activity of the vesicular monoamine transporter type 2, such that cytoplasmic dopamine concentration may be raised by the administration of exogenous dopamine in the culture medium [7,13–15].

Results

Dopamine increases the expression of α-synuclein to a threshold

To obtain a cellular model of α-synuclein overexpression, the human neuroblastoma cell line SH-SY5Y was stably transfected with the plasmid containing human α-synuclein cDNA (α-syn). As a control, we used SH-SY5Y cells stably transfected with the plasmid containing β-galactosidase cDNA (β-gal). Western blot analysis revealed a significant 1.6-fold increase in α-synuclein expression in α-syn cells with respect to β-gal cells (Fig. 1). The optimal concentration of dopamine to be used in the present study (0.250 mM; 70 ± 5% viability after 24 h for both β-gal and α-syn cells) was determined by the 3-(4,5-dimethylthiazol-2-yl)-2,5-diphenyltetrazolium bromide (MTT) assay (Fig. S1). Because dopamine upregulates α-synuclein expression [13], we measured the level of α-synuclein in α-syn cells with respect to β-gal cells in the presence of catalase only (cat) or in the presence of catalase and 0.250 mM dopamine for 24 h (DA). Dopamine treatment significantly increased the expression of α-synuclein in β-gal control cells but not in α-syn cells that already overexpress it as a consequence of transfection (Fig. 1).

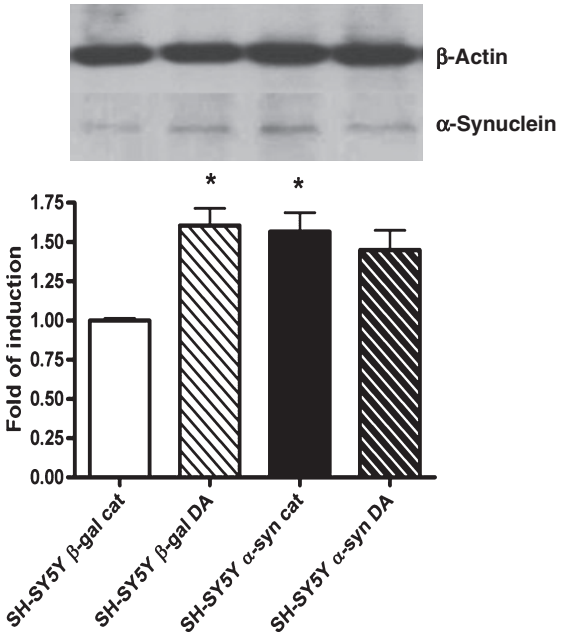

Fig. 1. Relative expression of α-synuclein in β-gal and α-syn cells in response to dopamine (DA) treatment. Results are indicated as the fold of induction relative to expression observed in β-gal cells treated with catalase (cat) (set to 1). Values (density of α-synuclein bands normalized to β-actin) are the mean ± SE of three independent experiments. $*P < 0.005$ versus β-gal cat cells.

Proteomics analysis reveals quantitative changes in 23 proteins

Proteomic investigations were conducted on β-gal and α-syn cells treated or not with dopamine, as described above. Statistical analysis, by two-way analysis of

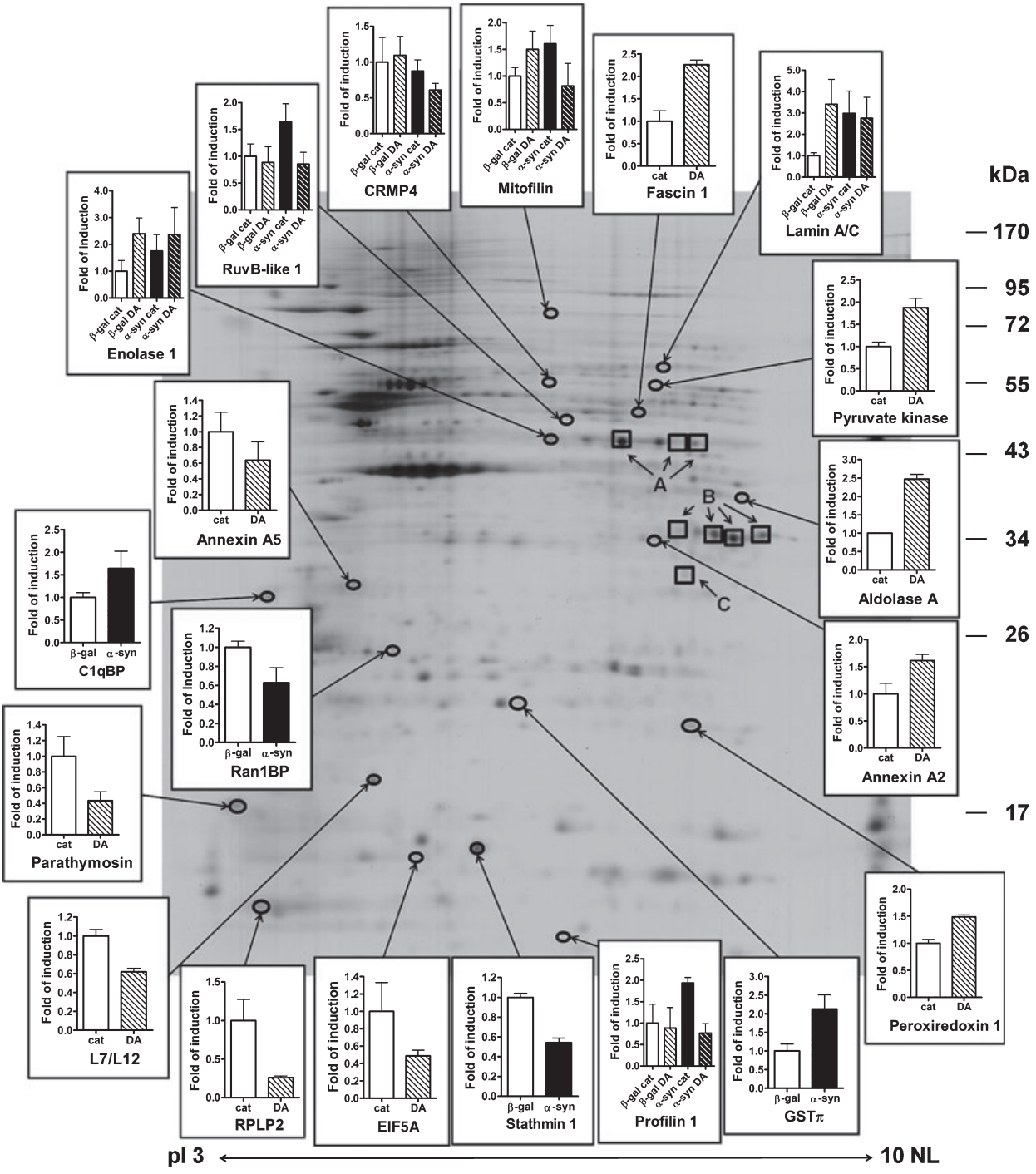

Fig. 2. A representative silver-stained 2-DE gel of proteins extracted from β-gal cells treated with catalase (cat). Qualitative differences are indicated by squares (A: ATP synthase α; B: GAPDH; C: VDAC2), whereas circles indicate spots whose levels change significantly. Insets report the relative change (i.e. fold of induction) with respect to the reference condition (β-gal, cat or β-gal cat) arbitrarily set to 1. Values are the mean ± SD of three different gels in four-bar histograms and of six gels in two-bars histograms. NL, nonlinear. For protein identification, see Table 1.

variance (ANOVA) of silver-stained gel images revealed 28 spots whose intensity was significantly different in at least one of the four groups considered (Fig. 2). Two groups of spots showing remarkable changes in the isoform pattern in the four conditions were easily assigned to glyceraldehyde 3-phosphate

Table 1. Identification of differentially expressed proteins. Protein spots in silver-stained gels were analyzed by ANOVA. DA, proteins that showed increased (↑) or decreased (↓) expression after dopamine treatment; α-syn, proteins that displayed increased (↑) or decreased (↓) expression as a consequence of α-synuclein overexpression; complex, proteins that displayed altered levels as a result of the association of dopamine treatment with α-synuclein overexpression (Fig. 2, insets).

Protein	Swiss-Protein ID	M_r (kDa)[a]	pI[a]	Identified peptides	Mascot score	Sequence coverage (%)	F[b]	P[b]	Observed change
RPLP2	P05387	11.7	4.42	4	268	53	8.41	0.020	DA ↓ × 3.9
Parathymosin	P20962	11.4	4.14	2	88	22	12.14	0.008	DA ↓ × 2.3
eIF5A isoform B	P63241	16.8	5.08	2	70	7	12.72	0.007	DA ↓ × 2.1
L7/L12, mitochondrial	P52815	21.4	5.37	3	140	11	9.28	0.016	DA ↓ × 1.6
Peroxiredoxin 1	Q06830	22.1	8.27	9	431	45	10.39	0.012	DA ↑ × 1.5
Annexin A5	Q6FHB3	35.9	4.83	13	720	52	6.72	0.032	DA ↓ × 1.6
Annexin A2	Q8TBV2	38.6	7.57	6	299	20	5.25	0.050	DA ↑ × 1.6
Aldolase A	P04075	39.3	8.34	5	210	20	36.86	0.001	DA ↑ × 2.5
Fascin 1	Q16658	54.5	6.84	7	333	16	5.88	0.042	DA ↑ × 2.3
Pyruvate kinase	P14618	57.8	7.95	12	521	29	7.22	0.028	DA ↑ × 1.9
VDAC-2	P45880.2	31.4	7.66	6	268	17	–[d]	–[d]	Absent in DA
Stathmin 1	P16949	17.3	5.76	7	305	32	15.24	0.005	α-Syn ↓ × 1.8
Ran1BP	P43487	23.2	5.19	4	206	21	10.38	0.012	α-Syn ↓ × 1.6
GSTπ	P09211	23.4	5.43	8	474	43	6.29	0.037	α-Syn ↑ × 2.1
C1qBP	Q07021	23.8	4.32	5	306	21	9.81	0.014	α-Syn ↑ × 1.6
Profilin 1	P07737	15.0	8.44	4	170	41	6.92	0.030	Complex
Enolase 1	P06733	47.1	7.01	8	481	24	6.94	0.03	Complex
RuvB-like 1	Q9Y265	50.2	6.02	10	343	28	11.58	0.009	Complex
CRMP4	Q14195	61.9	6.04	2	81	4	13.02	0.007	Complex
Lamin A/C	Q5TCJ3	72.2	6.40	11	536	22	10.91	0.011	Complex
Mitofilin, p32	Q16891	83.7	6.08	5	241	9	12.10	0.008	Complex
GAPDH	P04406	35.9	8.58	–[c]	–[d]	–[d]	–[d]	–[d]	Change in pattern
ATP synthase α	P25705	55.2	8.28	–[c]	–[d]	–[d]	–[d]	–[d]	Change in pattern

[a] Theoretical values. [b] F and P refer to ANOVA. [c] Identified from SWISS 2D-PAGE database. [d] Not applicable.

dehydrogenase and to mitochondrial ATP synthase α subunit by comparison with 2D electrophoresis (2-DE) maps available in the SWISS 2D-PAGE database (http://www.expasy.org). Additionally, 21 differentially expressed proteins were identified by LC-MS-MS (Table 1; for details on protein identification, see Table S1). After dopamine treatment, one spot completely disappeared (voltage-dependent anion channel 2; VDAC-2) and ten proteins [pyruvate kinase, 60S acidic ribosomal protein P2 (RPLP2), eukaryotic initiation factor 5A (eIF5A), parathymosin, L7/L12, annexin A2, annexin A5, aldolase A, fascin 1 and peroxyredoxin 1] displayed quantitative differences, regardless of whether or not α-synuclein was overexpressed (Fig. 2, insets; black versus white bars). Dopamine-responsive proteins were involved in protein synthesis, energetic metabolism, calcium-dependent phospholipid binding, cytoskeleton regulation, redox homeostasis and mitochondrial electrochemical balance. Regardless of dopamine treatment, overexpression of α-synuclein significantly affected the levels of four proteins [stathmin 1, glutathione *S*-transferase (GST)π, Ran 1 binding protein and C1q binding protein], related to cell signaling, apoptosis and cytoskeleton regulation (Fig. 2, insets; shaded versus white bars). On the other hand, six proteins were regulated in a more complex way (Fig. 2, insets; four-bar histograms), in that α-synuclein overexpression modulated the dopamine effect [profilin 1, enolase 1, RuvB-like 1, collapsin response mediator protein 4 (CRMP4) and lamin A/C, mitofilin]. These proteins deal with the regulation of the cytoskeleton, transcription and cell growth, signal transduction and mitochondrial trafficking.

Network enrichment highlights the involvement of the nuclear factor kappa B (NF-κB) pathway

Experimentally identified proteins were analyzed in terms of both interaction network and Gene Ontology (GO) classification enrichment using PPI SPIDER, a network enrichment algorithm based on known protein–protein physical interactions [16]. Figure 3 shows significant ($P < 0.05$) network models for proteins

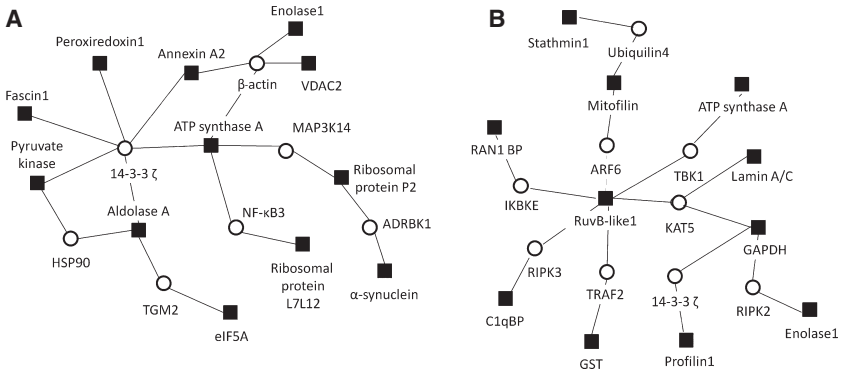

Fig. 3. Enriched protein networks. (A) Proteins that displayed significant changes after dopamine treatment. (B) Proteins that displayed significant changes as a consequence of α-synuclein overexpression or as a result of the association of dopamine treatment with α-synuclein overexpression. Experimentally identified proteins are indicated by filled squares. Open circles indicate common interactors as predicted by PPI SPIDER ($P < 0.05$).

that displayed significant changes after dopamine treatment, regardless of α-synuclein overexpression (Fig. 3A), and for proteins that displayed significant changes as a consequence of α-synuclein overexpression or as a result of the association of dopamine treatment with α-synuclein overexpression (Fig. 3B). The same analysis performed on all identified proteins was able to correctly cluster them in the two classes described above (data not shown). Statistically-significant ($P < 0.05$) functional association with GO classifications was obtained from PPI SPIDER starting from the proteins grouped as above (Tables S2 and S3).

In both cases, bioinformatic analysis revealed that the NF-κB pathway could be involved in determining the effects of dopamine treatment and α-synuclein overexpression. Accordingly, we transfected β-gal and α-syn cells with the pNF-κB-Luc reporter gene and measured the NF-κB-dependent luciferase activity (Fig. 4A). The basal activation of NF-κB was significantly reduced by 30% in α-syn cells with respect to β-gal cells, and the expression of the reporter gene in β-gal and α-syn cells was almost completely quenched after 24 h of dopamine treatment.

Because HSP70, a stress-inducible chaperonin, is known to inhibit NF-κB activation [17], we measured HSP70 levels in β-gal and α-syn cells treated, or not, with dopamine (0.250 mM, 24 h) by western blotting. Although HSP70 levels are similar in α-syn and β-gal cells, dopamine increases HSP70 levels, regardless of α-synuclein overexpression (Fig. 4B).

The suggestions obtained from enriched GO categories (Table S3) led us to evaluate apoptotic cell death in our experimental setting. The basal level of apoptotic cells is not significantly different in α-syn cells with respect to β-gal cells (in agreement with cell viability assays, see above). Dopamine triggers apoptotic cell death to the same extent in both α-syn and β-gal cells (Fig. 5). Remarkably, the percentage of necrotic cells also was not significantly affected by α-synuclein overexpression (Fig. S2).

Discussion

Proteins differentially expressed in this model are individually linked to PD

Most of the identified proteins may be linked to different pathogenetic mechanisms in PD, either specific or associated with generic stress conditions. Higher glycolytic activity is shown by higher aldolase A, enolase 1 and pyruvate kinase levels, together with a lower parathymosin level [18]. However, quantitative alterations of glycolytic enzymes are frequently observed after a generic stress event [19]. Qualitative variations of ATP synthase A and glyceraldehyde 3-phosphate dehydrogenase do not involve significant changes in total protein level, but rather a rearrangement of the isoform pattern. This finding could also reflect a proteome adaptation as a response to perturbation of protein levels caused by stimuli of different origin [20]. In parallel, proteins involved in protein synthesis (i.e. eIF5A, RPLP2 and its mitochondrial paralog L7/L12) were less abundant after dopamine treatment, suggesting attenuated translation at both cytoplasmic and mitochondrial levels under cellular stress conditions [21]. Upregulation of peroxyredoxin 1 is in keeping with increased reactive oxygen species production by dopamine oxidation that activates apoptosis and induces the synthesis of antioxidants [22].

Alterations in mitochondrial proteins, on the other hand, are specifically linked to one of the major pathogenetic mechanisms of PD [5]. Worthy of note is the complete disappearance of the VDAC-2 upon dopamine treatment. This porin of the outer mitochondrial membrane regulates mitochondrial Ca^{2+} homeostasis and mitochondrial-dependent cell death, which are major pathogenetic factors in PD [23,24]. The changes observed for mitofilin and mitochondrial C1q binding protein also suggest mitochondrial impairment. Interestingly, mitofilin is covalently modified by dopamine oxidation products [25].

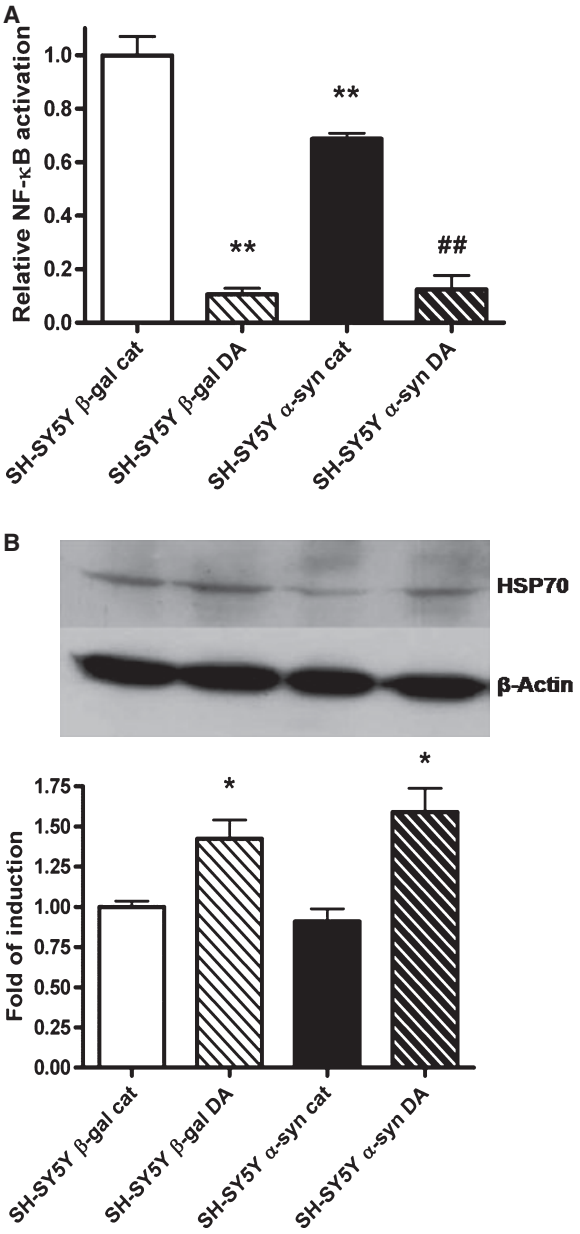

Fig. 4. Activation of the NF-κB pathway. (A) NF-κB activity measured by luciferase gene reporter assay after 24 h dopamine treatment (DA) relative to β-gal cells treated with catalase (β-gal cat, set to 1). $^{**}P < 0.001$ versus β-gal cat cells. $^{\#\#}P < 0.001$ versus α-syn cat cells. (B) Expression of the NF-κB regulator HSP-70 relative to expression observed in β-gal cat cells (set to 1). $^{*}P < 0.005$ versus β-gal cat cells. Values are the mean ± SE of three independent experiments.

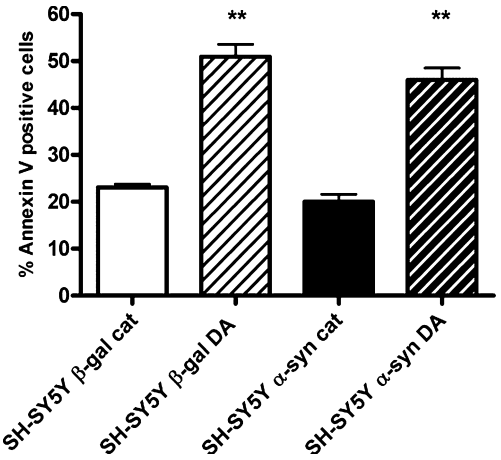

Fig. 5. Induction of apoptosis. Apoptotic β-gal and α-syn cells are measured as a percentage of annexin V positive cells in response to dopamine treatment DA. $^{**}P < 0.001$ DA versus cat cells. Values are the mean ± SE of three independent experiments.

Alterations in either cytoskeleton components or regulatory proteins were suggested to be linked to early stages of PD pathogenesis [26]. Interestingly, in our model, dopamine induces an increase of the actin bundles regulator fascin 1 [27] and discordant changes of two calcium-dependent, actin-associated proteins (annexins A2 and A5), both regulating membrane dynamics, cell migration, proliferation and apoptosis [28]. Recently, a role for α-synuclein in actin dynamics has been suggested [29]. Overexpression of α-synuclein definitely affects the cytoskeletal proteins necessary for neuronal differentiation and synaptic plasticity, such as profilin 1 [30], stathmin 1 [31] and lamin A/C [32]. Lamin levels could also change in response to oxidative stress conditions [33].

GSTπ, whose levels are increased in α-syn cells, may play an important role in modulating the progression of PD [34], and a GSTπ polymorphism is associated with PD in a *Drosophila* model expressing mutant parkin [35]. Moreover, its expression is responsible for nigral neuron sensitivity in an experimental model of PD [36] and quantitative changes in its levels were observed in SNpc specimens of PD patients by proteome analysis [37].

Eventually, three proteins have shed light on the Wnt/β-catenin pathway and its regulatory kinase glycogen synthase kinase-3β (GSK-3β). Following a Wnt signal, β-catenin is imported into the nucleus through RanGTP-dependent transport and activates the transcription of target genes by recruiting other factors such as the histone acetyltransferase RuvB-like 1 (Tip49/pontin). In the absence of a Wnt signal, β-catenin is targeted to degradation by phosphorylation by GSK-3β [38]. Levels of the RAN binding protein 1 were reduced in α-syn cells with respect to β-gal cells and RuvB-like 1 is upregulated in α-syn cells in the absence of dopamine. CRMP4, a member of a family of neuron-enriched proteins that regulate neurite

outgrowth and growth cone dynamics, is significantly reduced in α-syn cells. Interestingly, CRMP4 is also a substrate of GSK-3β [39]. Such evidence is in keeping with the recent description of a functional link between α-synuclein and GSK-3β activation [40].

Validation of proteomic data through an enriched network model

Although the involvement of most identified proteins with PD pathogenesis is an interesting result *per se*, we aimed to build a single, representative network that possibly grouped together all the proteins differentially expressed. Instead of validating every single protein by western blotting, we applied a different approach by searching for known physical interactions between the identified proteins, aiming to validate the body of the results as a whole. Unexpectedly, all proteins were included in two different networks and proteins responding to dopamine treatment only segregated from those showing a response to α-synuclein overexpression alone or in combination with dopamine treatment. The network enrichment procedure suggested a potential involvement of the NF-κB pathway and of apoptosis regulation. Confirming this suggestion, we observed experimentally that dopamine quenched NF-κB activation both in β-gal and α-syn cells similar to that reported for the PD-related neurotoxin MPP^+ [41]. Increased levels of the molecular chaperone HSP70 observed in response to dopamine could contribute to the inhibition of NF-κB [17]. Because the upregulation of HSP70 is only observed after dopamine treatment, the inhibition of NF-κB activity by α-synuclein overexpression should be linked to a different pathway (e.g. to the increase of GSK-3β activity), as was recently suggested [42]. It should be noted, however, that the NF-κB pathway is less active in all the experimental conditions where higher levels of α-synuclein are present, either as a consequence of transfection or of dopamine treatment (Fig. 1), suggesting that α-synuclein could at least contribute to the deactivation of this cascade.

Dopamine is known to induce apoptosis [43] and the results obtained in the present study are in agreement with this finding (Fig. 5). Although both anti-apoptotic and pro-apoptotic properties were attributed to α-synuclein [8,43], we did not observe any significant effect as a result of α-synuclein overexpression on the percentage of apoptotic cells. This finding suggests that a 60% increase of the α-synuclein level does not exert any apoptotic action by itself; rather, it could represent a threshold value that discriminates protective from toxic effects [8].

Conclusions

In conclusion, the proteomic analysis reported in the present study links dopamine toxicity to specific cellular processes such as cytoskeleton structure and regulation, mitochondrial function, energetic metabolism, protein synthesis and neuronal plasticity. From the consequent network enrichment procedure we focused on NF-κB activation, a transcription factor that regulates neuronal survival [44], and experimentally observed its quenching. These aspects are particularly relevant for an understanding of the biochemical pathways involved in PD neurodegeneration. Indeed, the triggers leading to the specific death of dopaminergic neurons of SNpc, as well as the proteins altered during the process, are still not well understood. Most likely, the main players in determining the sensitivity of dopaminergic neurons are altered dopamine homeostasis and α-synuclein misregulation. The analysis reported in the present study highlights the proteome alteration resulting from these pathogenetic mechanisms. Thus, by combining an experimental and computational approach, we completely fulfill the expectations for proteomics with respect to generating new hypotheses. Therefore, each element arising from the present study could represent a valuable starting-point for focused investigations aiming to better understand the key issues of PD pathogenesis.

Materials and methods

Cells

Human neuroblastoma SH-SY5Y cells were cultured in 5% CO_2 humidified atmosphere at 37 °C in high-glucose DMEM with 10% fetal bovine serum, 100 $U{\cdot}mL^{-1}$ penicillin, 100 $\mu g{\cdot}mL^{-1}$ streptomycin and 2 mM L-glutamine. All cell culture media and reagents were from PAA (Pasching, Austria).

As previously described [7], SH-SY5Y cells were transfected with the pcDNA-Syn plasmid containing the complete human wild-type α-synuclein coding sequence (amino acids 1–140) into the mammalian expression vector pcDNA3.1 (Invitrogen Ltd, Paisley, UK) or with the pcDNA-β-gal plasmid containing the β-galactosidase coding sequence as control. α-Synuclein-expressing cells (α-syn) and control cells (β-gal) were expanded in the presence of 200 $\mu g{\cdot}mL^{-1}$ geneticin. The cells rescued after selection were maintained as lines. Intentionally, cell lines were not cloned. This avoided working with only a few clones but, instead, resulted in an ensemble average of different clones.

Cell viability

The dopamine effect on cell viability was assessed by the MTT assay using the Celltiter 96 nonradioactive cell proliferation assay (Promega, Madison, WI, USA) in accordance with the manufacturer's instructions. Cells were exposed for 24 h to different dopamine concentrations (0.125–1.00 mM) in the presence of 700 $U \cdot mL^{-1}$ catalase to eliminate aspecific effects as a result of H_2O_2 arising from dopamine auto-oxidation [45]. A_{570} was monitored with a Universal Microplate reader Model 550 (Bio-Rad, Hercules, CA, USA). All experiments were run in triplicate.

2-DE electrophoresis and statistical analysis

α-Syn and β-gal cells treated or not with 0.250 mM dopamine in the presence of catalase for 24 h were collected by centrifugation, lysed with 200 μL of lysis solution [7 M urea, 2 M thiourea, 4% (w/v) CHAPS, 0.5 μL of protease inhibitor mix] and centrifuged (13000 ***g*** for 30 min at 10 °C). Proteins were collected in the supernatant and their concentration was determined using the Bio-Rad Protein Assay (Bio-Rad). All experiments were run in triplicate. In this way, three independent samples were obtained for each condition (α-syn and β-gal cells, regardless of whether or not they were treated with dopamine).

2-DE was performed according to Görg *et al*. [46], with minor modifications. Samples (approximately 200 μg) were diluted to 250 μL with a buffer containing 7 M urea, 2 M thiourea, 4% CHAPS, 0.5% IPG buffer 3–10, 2 mM tributylphosphine and traces of bromophenol blue, and loaded on 13 cm IPG DryStrips with a nonlinear 3–10 pH gradient by in-gel rehydration (1 h at 0 V, 10 h at 50 V). Isoelectrofocussing was performed at 20 °C on IPGphor (GE Healthcare, Little Chalfont, UK) with the schedule: 2 h at 200 V, 2 h linear gradient to 2000 V, 2 h at 2000 V, 1 h of linear gradient to 5000 V, 2 h at 5000 V, 2 h linear gradient to 8000 V and 2 h and 30 min at 8000 V. IPG strips were then equilibrated for 2 × 30 min in 50 mM Tris-HCl (pH 8.8), 6 M urea, 30% glycerol, 2% SDS and traces of bromophenol blue containing 1% dithiothreitol for the first equilibration step and 2.5% iodoacetamide for the second one. SDS/PAGE was performed using 13%, 1.5 mm thick separating polyacrylamide gels without stacking gel, using Hoefer SE 600 system (GE Healthcare). The second dimension was carried out at 45 mA per gel at 18 °C. Molecular weight marker proteins (11–170 kDa; Fermentas, Burlington, Canada) were used for calibration.

The 12 gels (three for each experimental condition) were stained according to MS-compatible silver staining method [47], scanned with an Epson Perfection V750 Pro transmission scanner (Epson, Nagano, Japan) and analyzed with IMAGEMASTER 2D PLATINUM software, version 5.0 (GE Healthcare). Spots were detected automatically by the software and manually refined; gels were then matched and the resulting clusters of spots confirmed manually. Unmatched spots among the experimental groups were considered as qualitative differences. Synthetic images ('average gels') comprising spots present in all gels of each experimental condition were built and then compared; spots were quantified on the basis of their relative volume (spot volume normalized to the sum of the volumes of all the representative spots) and those that consistently and significantly varied among the different populations were identified by two-way ANOVA analysis with a threshold of $P \leq 0.05$ using STATISTIXL software (http://www.statistixl.com). Folds of induction were calculated with respect to the reference condition (β-gal, cat or β-gal cat) arbitrarily set to 1. Where one of the experimental conditions did not affect significantly the protein level, the relative datasets were joined (six values, two experimental conditions).

LC-MS-MS analysis for protein identification

Silver-stained spots were manually excised and destained (1 × 10 min 50 μL of $K_3[Fe(CN)_6]$ 30 mM and $Na_2S_2O_3$ 100 mM; 6 × 10 min 100 μL of deionized water; 1 × 20 min 100 μL of NH_4HCO_3 200 mM; 1 × 20 min 100 μL of deionized water), dehydrated with acetonitrile (1 × 40 min 100 μL) and then dried at 37 °C by vacuum centrifugation. The gel pieces were then swollen in 10 μL of digestion buffer containing 50 mM NH_4HCO_3 and 12.5 $ng \cdot \mu L^{-1}$ modified porcine trypsin (sequencing grade; Promega). After 10 min, 30 μL of 50 mM NH_4HCO_3 were added to the gel pieces and digestion allowed to proceed at 37 °C overnight. The supernatants were collected and peptides were extracted in an ultrasonic bath for 10 min [twice: 100 μL of 50% acetonitrile, 50% H_2O, 1% formic acid (v/v); once: 50 μL of acetonitrile]. All the supernatants were collected in the same tube, dried by vacuum centrifugation and dissolved in 20 μL of 2% acetonitrile, 0.1% of formic acid in water.

Peptide mixtures were separated by using a nanoflow-HPLC system (series 1200; Technologies Agilent, Santa Clara, CA, USA). A sample volume of 10 μL was loaded onto a 2 cm fused silica pre-column (inner diameter 75 μm, outer diameter 375 μm) at a flow rate of 2 $\mu L \cdot min^{-1}$. Peptides were eluted at a flow rate of 200 $nL \cdot min^{-1}$ with a linear gradient from Solution A (2% acetonitrile; 0.1% formic acid) to 50% of Solution B (98% acetonitrile; 0.1% formic acid) in 40 min over the pre-column in-line with a homemade 15 cm resolving column (inner diameter 75 μm, outer diameter 375 μm; Zorbax 300-SB C18; Agilent Technologies). Peptides were eluted directly into a Esquire 6000 Ion Trap mass spectrometer (Bruker-Daltonik, Bremen, Germany). Capillary voltage was 1.5–2 kV and a dry gas flow rate of 10 $L \cdot min^{-1}$ was used with a temperature of 230 °C. The scan range was 300–1800 *m/z*. The tandem mass spectra were annotated and peak list files were generated, commonly referred to as MGF files, by running DATAANALYSIS, version 3.2 (Bruker-Daltonik) using default parameters. Protein identification was manually performed

by searching the National Center for Biotechnology Information nonredundant database (NCBInr 20081021; 709593 sequences searched) using MASCOT MS/MS ION SEARCH software, version 27 (http://www.matrixscience.com). The parameters set were: enzyme trypsin, complete carbamidomethylation of cysteines and partial oxidation of methionines, peptide mass tolerance ±0.9 Da, fragment mass tolerance ±0.9 Da, missed cleavages 2, species restriction to mammals. All identified proteins are human and have a MASCOT score greater than 69, corresponding to a statistically significant ($P < 0.05$) confident identification. Among the positive matches, only protein identifications based on at least two different non-overlapping peptide sequences of more than six amino acids and with a mass tolerance < 0.9 Da were accepted (Table S1).

Bioinformatics enrichment and network clustering

Identified proteins were clustered in two groups. The first one corresponds to proteins that displayed significant changes in their levels after dopamine treatment ('DA' in Table 1). The second one groups together proteins that show quantitative alterations in response to α-synuclein overexpression ('α-Syn' in Table 1), or that differentially respond to dopamine exposure as a function of α-synuclein overexpression ('Complex' in Table 1). Lists were fed to PPI SPIDER (http://mips.helmholtz-muenchen.de/proj/ppispider/) aiming to determine a statistically significant interaction network, as well as statistically significant functional association with GO classifications [16].

Western blotting

Expression of α-synuclein and HSP70 was determined by western blotting. Proteins (80 μg) were extracted in RIPA buffer (25 mM Tris-HCl, pH 7.4, 0.15 M NaCl, 0.1% SDS, 1% Triton X-100, 1% sodium deoxycholate), resolved by SDS/PAGE on a 16% polyacrylamide gel and then transferred to a poly(vinylidene difluoride) membrane (Roth, Karlsruhe, Germany) at 25 V for 2 h. The membrane was incubated with mouse anti-α-synuclein (BD Transduction Laboratories, Franklin Lakes, NJ, USA), mouse anti-HSP70 (Zymed Laboratories, San Francisco, CA, USA) or mouse anti-β-actin (GeneTex, Irvine, CA, USA) monoclonal antibodies diluted 1 : 1000 in 5% nonfat dry milk in NaCl/Tris-Tween (10 mM Tris HCl, pH 8, 150 mM NaCl, 0.05% Tween 20) for 1.5 h at room temperature. Protein bands were visualized using a peroxidase-conjugated anti-mouse IgG secondary antibody (GeneTex) and the ECL plus western blotting detection system (Millipore, Billerica, MA, USA). Relative levels of α-synuclein and HSP70 were calculated by densitometric analysis (IMAGEJ software; http://rsb.info.nih.gov/ij) and normalized to β-actin. All experiments were run in triplicate.

Apoptosis analysis

The induction of apoptotic cell death was analyzed by flow cytometry with the Annexin V-FITC apoptosis detection kit (Becton-Dickinson, Franklin Lakes, NJ, USA). Briefly, cells were resuspended (1×10^6 cells·mL^{-1}) in binding buffer; 1×10^5 cells were incubated with Annexin V-FITC and propidium iodide for 15 min at room temperature in the dark. Samples properly diluted were analyzed with a FACSCalibur flow cytometer (Becton-Dickinson) equipped with a 15 mW, 488 nm, air-cooled argon ion laser. At least 10 000 events were analyzed for each sample and data were processed using CellQuest software (Becton-Dickinson). Fluorescent emission of propidium iodide and Annexin V-FITC were collected through a 575 and a 530/30 band-pass filter, respectively. The percentage of apoptotic cells in each sample was determined based on the fraction of annexin V positive cells. All experiments were run in triplicate.

Transient transfection and luciferase gene reporter assay

β-Gal and α-syn cells (60% confluent in six-well plates) were transfected with pNF-κB-Luc plasmid (Stratagene, Santa Clara, CA, USA) (150 ng·well^{-1}) and phRL-CMV, containing Renilla luciferase cDNA (5 ng·well^{-1}), using Lipofectamine and OptiMEM medium (Invitrogen, Carlsbad, CA, USA). In pNF-κB-Luc the expression of the firefly luciferase is controlled by a synthetic promoter containing five NF-κB binding sites. After 7 h of incubation, the transfection mixture was replaced with complete DMEM containing, or not, 0.250 mM dopamine, in the presence of 700 U·mL^{-1} catalase. Cells were harvested after 24 h, lysed and the cell lysates were tested for luciferase activities by using the Dual-Luciferase reporter assay system (Promega) in accordance with the manufacturer's instructions. Experiments were performed in duplicate and repeated three times with almost identical results being obtained, indicating statistical significance. NF-κB-dependent luciferase activity was normalized to the Renilla luciferase activity present in each sample.

Acknowledgements

The authors gratefully acknowledge Professor Roberto Accolla and Professor Piero Canonico for their helpful discussions.

References

1 Thomas B & Beal MF (2007) Parkinson's disease. *Hum Mol Genet* **16** Spec. No. 2, R183–R194.
2 Devine MJ & Lewis PA (2008) Emerging pathways in genetic Parkinson's disease: tangles, Lewy bodies and LRRK2. *FEBS J* **275**, 5748–5757.

3 Fasano M, Bergamasco B & Lopiano L (2006) Modifications of the iron-neuromelanin system in Parkinson's disease. *J Neurochem* **96**, 909–916.
4 Fasano M & Lopiano L (2008) Alpha-synuclein and Parkinson's disease: a proteomic view. *Expert Rev Proteomics* **5**, 239–248.
5 Henchcliffe C & Beal MF (2008) Mitochondrial biology and oxidative stress in Parkinson disease pathogenesis. *Nat Clin Pract Neurol* **4**, 600–609.
6 Lesage S & Brice A (2009) Parkinson's disease: from monogenic forms to genetic susceptibility factors. *Hum Mol Genet* **18**, R48–R59.
7 Colapinto M, Mila S, Giraudo S, Stefanazzi P, Molteni M, Rossetti C, Bergamasco B, Lopiano L & Fasano M (2006) Alpha-synuclein protects SH-SY5Y cells from dopamine toxicity. *Biochem Biophys Res Commun* **349**, 1294–1300.
8 Cookson MR (2006) Hero versus antihero: the multiple roles of alpha-synuclein in neurodegeneration. *Exp Neurol* **199**, 238–242.
9 Quilty MC, King AE, Gai WP, Pountney DL, West AK, Vickers JC & Dickson TC (2006) Alpha-synuclein is upregulated in neurones in response to chronic oxidative stress and is associated with neuroprotection. *Exp Neurol* **199**, 249–256.
10 Lee HG, Zhu X, Takeda A, Perry G & Smith MA (2006) Emerging evidence for the neuroprotective role of alpha-synuclein. *Exp Neurol* **200**, 1–7.
11 Fasano M, Bergamasco B & Lopiano L (2007) The proteomic approach in Parkinson's disease. *Proteomics Clin Appl* **1**, 1428–1435.
12 Fasano M, Alberio T & Lopiano L (2008) Peripheral biomarkers of Parkinson's disease as early reporters of central neurodegeneration. *Biomarker Med* **2**, 465–478.
13 Gómez-Santos C, Ferrer I, Santidrian AF, Barrachina M, Gil J & Ambrosio S (2003) Dopamine induces autophagic cell death and alpha-synuclein increase in human neuroblastoma SH-SY5Y cells. *J Neurosci Res* **73**, 341–350.
14 Gómez-Santos C, Barrachina M, Giménez-Xavier P, Dalfó E, Ferrer I & Ambrosio S (2005) Induction of C/EBP beta and GADD153 expression by dopamine in human neuroblastoma cells. Relationship with alpha-synuclein increase and cell damage. *Brain Res Bull* **65**, 87–95.
15 Gómez-Santos C, Francisco R, Giménez-Xavier P & Ambrosio S (2007) Dopamine induces TNFalpha and TNF-R1 expression in SH-SY5Y human neuroblastoma cells. *Neuroreport* **18**, 1725–1728.
16 Antonov AV, Dietmann S, Rodchenkov I & Mewes HW (2009) PPI spider: A tool for the interpretation of proteomics data in the context of protein-protein interaction networks. *Proteomics* **9**, 2740–2749.
17 Salminen A, Paimela T, Suuronen T & Kaarniranta K (2008) Innate immunity meets with cellular stress at the IKK complex: regulation of the IKK complex by HSP70 and HSP90. *Immunol Lett* **117**, 9–15.
18 Brand IA & Heinickel A (1991) Key enzymes of carbohydrate metabolism as targets of the 11.5-kDa Zn(2+)-binding protein (parathymosin). *J Biol Chem* **266**, 20984–20989.
19 Petrak J, Ivanek R, Toman O, Cmejla R, Cmejlova J, Vyoral D, Zivny J & Vulpe CD (2008) Déjà vu in proteomics. A hit parade of repeatedly identified differentially expressed proteins. *Proteomics* **8**, 1744–1749.
20 Mao L, Zabel C, Herrmann M, Nolden T, Mertes F, Magnol L, Chabert C, Hartl D, Herault Y, Delabar JM *et al*. (2007) Proteomic shifts in embryonic stem cells with gene dose modifications suggest the presence of balancer proteins in protein regulatory networks. *PLoS ONE* **2**, e1218.
21 Shenton D, Smirnova JB, Selley JN, Carroll K, Hubbard SJ, Pavitt GD, Ashe MP & Grant CM (2006) Global translational responses to oxidative stress impact upon multiple levels of protein synthesis. *J Biol Chem* **281**, 29011–29021.
22 Lev N, Ickowicz D, Barhum Y, Lev S, Melamed E & Offen D (2009) DJ-1 protects against dopamine toxicity. *J Neural Transm* **116**, 151–160.
23 Celsi F, Pizzo P, Brini M, Leo S, Fotino C, Pinton P & Rizzuto R (2009) Mitochondria, calcium and cell death: a deadly triad in neurodegeneration. *Biochim Biophys Acta* **1787**, 335–344.
24 Chan CS, Gertler TS & Surmeier DJ (2009) Calcium homeostasis, selective vulnerability and Parkinson's disease. *Trends Neurosci* **32**, 249–256.
25 Van Laar VS, Mishizen AJ, Cascio M & Hastings TG (2009) Proteomic identification of dopamine-conjugated proteins from isolated rat brain mitochondria and SH-SY5Y cells. *Neurobiol Dis* **34**, 487–500.
26 Xun Z, Sowell RA, Kaufman TC & Clemmer DE (2007) Lifetime proteomic profiling of an A30P alpha-synuclein *Drosophila* model of Parkinson's disease. *J Proteome Res* **6**, 3729–3738.
27 Tseng Y, Kole TP, Lee JS, Fedorov E, Almo SC, Schafer BW & Wirtz D (2005) How actin crosslinking and bundling proteins cooperate to generate an enhanced cell mechanical response. *Biochem Biophys Res Commun* **334**, 183–192.
28 Monastyrskaya K, Babiychuk EB & Draeger A (2009) The annexins: spatial and temporal coordination of signaling events during cellular stress. *Cell Mol Life Sci* **66**, 2623–2642.
29 Sousa VL, Bellani S, Giannandrea M, Yousuf M, Valtorta F, Meldolesi J & Chieregatti E (2009) α-Synuclein and its A30P mutant affect actin cytoskeletal structure and dynamics. *Mol Biol Cell* **20**, 3725–3739.
30 Birbach A (2008) Profilin, a multi-modal regulator of neuronal plasticity. *Bioessays* **30**, 994–1002.

31 Andersen SS (2000) Spindle assembly and the art of regulating microtubule dynamics by MAPs and Stathmin/Op18. *Trends Cell Biol* **10**, 261–267.
32 Broers JL, Ramaekers FC, Bonne G, Yaou RB & Hutchison CJ (2006) Nuclear lamins: laminopathies and their role in premature ageing. *Physiol Rev* **86**, 967–1008.
33 Nakamura M, Morisawa H, Imajoh-Ohmi S, Takamura C, Fukuda H & Toda T (2009) Proteomic analysis of protein complexes in human SH-SY5Y neuroblastoma cells by using blue-native gel electrophoresis: an increase in lamin A/C associated with heat shock protein 90 in response to 6-hydroxydopamine-induced oxidative stress. *Exp Gerontol* **44**, 375–382.
34 Shi M, Bradner J, Bammler TK, Eaton DL, Zhang J, Ye Z, Wilson AM, Montine TJ, Pan C & Zhang J (2009) Identification of glutathione S-transferase pi as a protein involved in Parkinson disease progression. *Am J Pathol* **175**, 54–65.
35 Whitworth AJ, Theodore DA, Greene JC, Benes H, Wes PD & Pallanck LJ (2005) Increased glutathione S-transferase activity rescues dopaminergic neuron loss in a *Drosophila* model of Parkinson's disease. *Proc Natl Acad Sci USA* **102**, 8024–8029.
36 Smeyne M, Boyd J, Raviie Shepherd K, Jiao Y, Pond BB, Hatler M, Wolf R, Henderson C & Smeyne RJ (2007) GSTpi expression mediates dopaminergic neuron sensitivity in experimental parkinsonism. *Proc Natl Acad Sci USA* **104**, 1977–1982.
37 Werner CJ, Heyny-von Haussen R, Mall G & Wolf S (2008) Proteome analysis of human substantia nigra in Parkinson's disease. *Proteome Sci* **6**, 8.
38 Takashima A (2009) Drug development targeting the glycogen synthase kinase-3beta (GSK-3beta)-mediated signal transduction pathway: role of GSK-3beta in adult brain. *J Pharmacol Sci* **109**, 174–178.
39 Cole AR, Causeret F, Yadirgi G, Hastie CJ, McLauchlan H, McManus EJ, Hernández F, Eickholt BJ, Nikolic M & Sutherland C (2006) Distinct priming kinases contribute to differential regulation of collapsin response mediator proteins by glycogen synthase kinase-3 *in vivo*. *J Biol Chem* **281**, 16591–16598.
40 Duka T, Duka V, Joyce JN & Sidhu A (2009) Alpha-synuclein contributes to GSK-3beta-catalyzed Tau phosphorylation in Parkinson's disease models. *FASEB J* **23**, 2820–2830.
41 Halvorsen EM, Dennis J, Keeney P, Sturgill TW, Tuttle JB & Bennett JB Jr (2002) Methylpyridinium (MPP(+))- and nerve growth factor-induced changes in pro- and anti-apoptotic signaling pathways in SH-SY5Y neuroblastoma cells. *Brain Res* **952**, 98–110.
42 Yuan Y, Jin J, Yang B, Zhang W, Hu J, Zhang Y & Chen NH (2008) Overexpressed alpha-synuclein regulated the nuclear factor-kappaB signal pathway. *Cell Mol Neurobiol* **28**, 21–33.
43 Cookson MR & van der Brug M (2008) Cell systems and the toxic mechanism(s) of alpha- synuclein. *Exp Neurol* **209**, 5–11.
44 Sarnico I, Lanzillotta A, Benarese M, Alghisi M, Baiguera C, Battistin L, Spano P & Pizzi M (2009) NF-kappaB dimers in the regulation of neuronal survival. *Int Rev Neurobiol* **85**, 351–362.
45 Blum D, Torch S, Nissou MF, Benabid AL & Verna JM (2000) Extracellular toxicity of 6-hydroxydopamine on PC12 cells. *Neurosci Lett* **283**, 193–196.
46 Görg A, Obermaier C, Boguth G, Harder A, Scheibe B, Wildgruber R & Weiss W (2000) The current state of two-dimensional electrophoresis with immobilized pH gradients. *Electrophoresis* **21**, 1037–1053.
47 Gromova I & Celis JE (2006) Protein detection in gels by silver staining: A procedure compatible with mass-spectrometry. In *Cell Biology: A Laboratory Handbook* (Celis JE, Carter N, Hunter T, Simons K, Small JV & Shotton D eds), pp. 219–224. Academic Press, New York.

Supporting information

The following supplementary material is available:
Fig. S1. Dose-dependent dopamine effect on cell viability measured by the MTT assay.
Fig. S2. Percentage of propidium iodide positive β-gal and α-syn cells in response to dopamine treatment.
Table S1. MS/MS peptide sequence analysis of successfully identified proteins.
Table S2. Enriched GO categories starting from proteins that displayed significant changes after dopamine treatment, regardless of α-synuclein overexpression.
Table S3. Enriched GO categories starting from proteins that displayed significant changes after α-synuclein overexpression or in a more complex way.

This supplementary material can be found in the online version of this article.

Please note: As a service to our authors and readers, this journal provides supporting information supplied by the authors. Such materials are peer-reviewed and may be re-organized for online delivery, but are not copy-edited or typeset. Technical support issues arising from supporting information (other than missing files) should be addressed to the authors.